34th Annual International Conference of the IEEE EMBS
San Diego, California USA, 28 August - 1 September, 2012

Titanium-Based, Fenestrated, In-Plane Microneedles for Passive Ocular Drug Delivery

Omid Khandan, *Member, IEEE*, Amin Famili, Malik Y. Kahook, and Masaru P. Rao, *Member, IEEE*

Abstract— **Drug delivery to the eye remains a key challenge, due to limitations inherent to prevailing delivery techniques. For example, while topical delivery offers simplicity and safety, its efficacy is often limited by poor bioavailability, due to natural transport barriers and clearance mechanisms. Similarly, while intravitreal injections performed across the ocular tunic provide means for circumventing such limitations, non-negligible potential for retinal detachment and other complications adversely affects safety. Herein, we discuss our initial efforts to address these limitations through development of titanium-based microneedles (MNs) which seek to provide a safer, simpler, and more efficacious means of ocular drug delivery. Devices with in-plane geometry and through-thickness fenestrations that serve as drug reservoirs for passive delivery via diffusive transport from fast-dissolving coatings are demonstrated. Details regarding device design, fabrication, and mechanical testing are presented, as are results from preliminary coating characterization and insertion testing in *ex vivo* rabbit cornea.**

I. Introduction

A number of current and emerging pharmacological therapies offer means for slowing the progression of leading ocular diseases, such as age-related macular degeneration (AMD), glaucoma, and diabetic retinopathy, thus providing opportunity for preservation of sight in those so afflicted. However, treatment of these diseases is nonetheless hampered by limitations inherent to the techniques currently available for delivery of such therapies. For example, opportunity for delivery via systemic approaches (e.g., oral formulations or parenteral injections) is largely precluded by lack of specificity, which results in undesirable side effects and systemic toxicity. Topical delivery via eye drops allows better targeting and, as such, is used widely. However, this approach is highly inefficient and subject to poor patient compliance, due in part to required frequency of application. Moreover, inability to deliver sufficient concentrations to the back of the eye (e.g., the retina) also limits utility for treatment of posterior segment diseases (e.g., AMD). Delivery to the vitreous (i.e. interior of the eye) via intravitreal injection enables more efficient posterior segment targeting. However, this approach is associated with potential for retinal detachment and infection, which is exacerbated by the need for frequently recurring injections for the remainder of the patient's life, due to the short half-life of most current drugs. Requirement for administration by trained medical personnel also imposes significant burden on the healthcare system. Collectively, these limitations demonstrate that development of a safe, simple, and efficacious means for targeted and sustained ocular drug delivery remains a critical unmet need.

Motivated by the significance of this need, and its attendant market potential, a wide variety of alternative targeted delivery approaches are currently being explored by the academic and industrial research communities. Typically, these approaches seek to circumvent physiological transport barriers (e.g., via permeability enhancers or nanoparticle formulations) and/or achieve sustained delivery by increasing drug residence time (e.g., via drug-eluting contact lenses or implantable reservoirs). While many show potential for enhancing safety, simplicity, or efficacy, none address all requirements simultaneously.

Microneedles (MNs) offer significant promise for ocular drug delivery, due in large part to their diminutive size, which allows penetration into, but not through sclera or cornea. This provides a precise, minimally-invasive, and non-surgical means for depositing drugs within such tissues. In doing so, MNs enable circumvention of the epithelial transport barrier and conjunctival clearance mechanism, while also minimizing potential for retinal damage. This, therefore, provides opportunity for near-optimal balance of safety, simplicity, and efficacy. While MNs based on both passive [1] and active [2, 3] delivery approaches have been reported, the former may ultimately prove more advantageous for routine clinical use, due to lower complexity and cost. However, potential for clinical translation will be constrained by the limited drug loading capacity of devices demonstrated to date, since this necessitates use of excessively large MN arrays to deliver therapeutically-relevant dosages.

Herein, we discuss our initial efforts to address these limitations through development of titanium-based fenestrated MNs that maximize drug loading capacity per needle, thus minimizing the total number of needles required for delivery of desired dosages. Details regarding device design, fabrication, and mechanical testing are presented, as are results from preliminary coating characterization and insertion testing in *ex vivo* rabbit cornea.

O. Khandan is with the Department of Mechanical Engineering, University of California, Riverside, CA 92521 (e-mail: okhandan@engr.ucr.edu).

A. Famili is with the Department of Bioengineering, University of Colorado, Denver, CO 80217 (e-mail: amin.famili@ucdenver.edu).

M. Y. Kahook is an Associate Professor in the Department of Ophthalmology, University of Colorado School of Medicine, Aurora, CO 80045 (e-mail: malik.kahook@gmail.com).

M. P. Rao is an Assistant Professor in the Department of Mechanical Engineering, University of California, Riverside, CA 92521 (e-mail: mprao@engr.ucr.edu).

II. Device Design and Fabrication

A. Design

MNs produced in this study were designed for passive intracorneal and intrascleral delivery within a New Zealand rabbit model via diffusive transport from a fast-dissolving coating. As shown in Fig. 1, through-thickness fenestrations were defined to act as drug reservoirs, while a trussed structure was selected to maximize carrying capacity and maintain sufficient stiffness for insertion. Preliminary estimates suggest that these fenestrations may increase drug loading up to 5-fold relative to solid MNs of identical shank dimensions (Table 1). MNs with lengths ranging from 500 – 1500 µm, widths from 50 – 200 µm, thickness of 50 µm, and needle tip angle of 60° were developed. Since optimal designs for the intended applications have yet to be defined, the given variation of these parameters was reflective of the desire to eventually determine the most favorable combination that ensures reliable insertion, minimized trauma, and maximized drug loading capacity.

Finite element analyses (FEA) were performed for all design variants to evaluate buckling performance, since this was expected to be the primary failure mode during insertion. Analyses for both fixed-free and fixed-pinned end conditions were performed, since our earlier studies of related devices under similar loading suggested these would be appropriate for the current devices [4, 5].

B. Fabrication

MNs were fabricated from 50 µm thick Grade 1 CP Ti using the titanium inductively coupled plasma deep etch (TIDE) process [6]. Fig. 2 details the fabrication process, which began with deposition of a 3 µm PECVD SiO_2 etch mask, followed by lithographic patterning, dry etching of the mask, anisotropic through-etching of the underlying Ti using the TIDE process, and removal of the mask by dry etching. Fig. 3 shows a typical fenestrated Ti MN illustrating its diminutive size relative to a conventional 26 g stainless steel hypodermic needle commonly used for intravitreal injection.

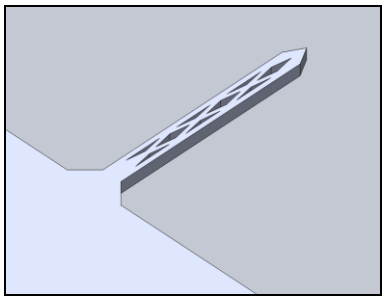

Fig. 1. Schematic illustration of a fenestrated Ti MN.

Table 1. Estimated increase in drug loading capacity for fenestrated Ti MNs relative to solid MNs of identical shank dimensions. Estimates are based upon assumption of complete fenestration filling and 1 µm global coating thickness.

		MN width [µm]			
		50	100	150	200
MN length [µm]	500	184%	210%	332%	412%
	1000	221%	247%	329%	518%
	1500	238%	293%	374%	526%

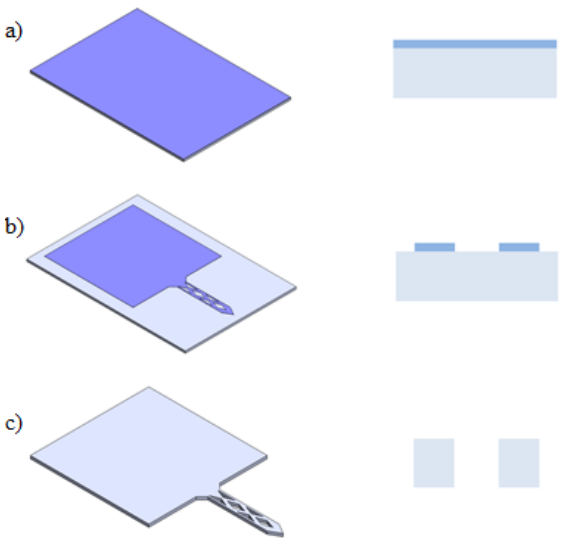

Fig. 2. Fabrication process for fenestrated Ti MNs: a) PECVD-based deposition of 3 µm SiO_2 layer on 50 µm thick Ti foil; b) Photo-lithographic patterning and dry etching of SiO_2 etch mask; and c) Ti DRIE followed by mask removal via dry etching.

C. Coating

Coating formulations were derived from earlier studies by others focused on coating of stainless steel MNs [7]. Aqueous formulations were prepared using 5% polyvinylpyrrolidone (PVP), 0.5% Lutrol F-68, and 0.1% Rhodamine B (all w/v %), since these were shown to provide a good balance of viscosity and wettability (on steel), while also allowing complete dissolution in water within 15 s. PVP served as a viscosity enhancer, while Lutrol served as a surfactant to reduce surface tension. Rhodamine B served as a model small molecule drug and provided means for characterizing coating performance via fluorescence microscopy. Oxygen plasma activation of the MNs was performed prior to coating to increase surface energy and wettability. MNs were manually dip coated and dried overnight at room temperature.

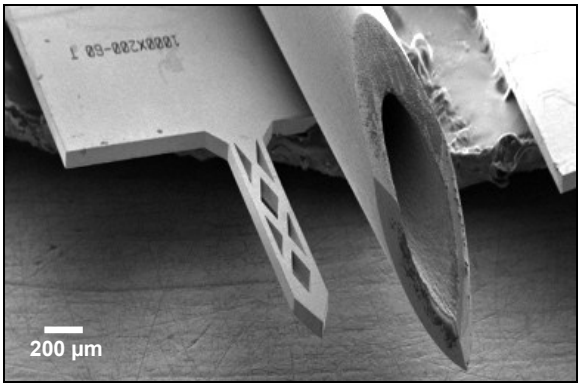

Fig. 3. Scanning electron micrograph of fenestrated Ti MN (1000 x 200 x 50 μm^3) and 26 g hypodermic needle (463 µm O.D.).

III. Device Characterization

A. Mechanical Testing

Buckling behavior was assessed by longitudinal uniaxial compression of the MNs onto a hard surface using a nanoindenter under displacement-controlled conditions. A minimum of 15 MNs were tested for each design variant. The critical buckling load ($P_{critical}$) for each design variant was extracted from the recorded load-displacement data.

B. MN Coating Characterization

Preliminary characterization of the MN coating process was performed using fluorescence microscopy, with a primary focus on qualitative evaluation of coating uniformity and fenestration filling.

C. Ex Vivo Tissue Insertion

Preliminary histological characterization of MN insertion was performed using excised rabbit cornea. Prior to testing, tissue specimens were submerged in physiological saline for 5 min, dried, and mounted on a hemispherical aluminum block with radius of curvature approximating that of the rabbit eye. MNs were manually inserted and then removed. Immediately afterwards, the corneas were cut close to the insertion site, embedded in paraffin wax, sectioned into 10 µm sagittal slices, and baked to remove residual paraffin. Hematoxylin-eosin stain was then performed, followed by examination by stereo microscopy.

IV. Results and Discussion

A. Mechanical Testing and FEA

Fig. 4 shows experimentally measured load-displacement data for select MN design variants, where $P_{critical}$ is identified as the maximum load for each test. For most design variants, measured $P_{critical}$ values exceed those reported for scleral insertion of 31 g needles [8]. This, therefore, suggests that the fenestrated Ti MNs possess sufficient stiffness for intrascleral penetration *in vivo*, particularly since lower insertion loads are expected for the MNs, due to their smaller cross section areas. Fig. 5 shows that measured $P_{critical}$ values fall within the bounds predicted by FEA. This agreement

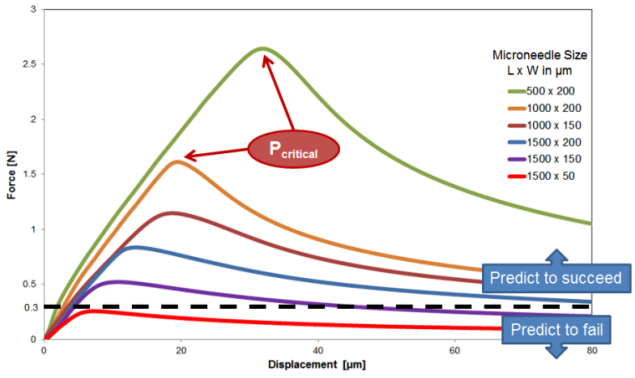

Fig. 4. Load-displacement data for select fenestrated Ti MN geometries under axial compression. Dashed line represents scleral penetration force reported for 31 g hypodermic needles [8].

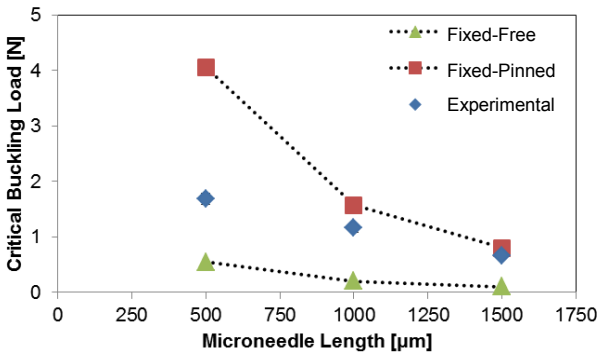

Fig. 5. Measured and FEA-predicted critical buckling loads for fenestrated Ti MNs with 50 µm thickness, 150 µm width, and varying lengths. Experimental data points represent average of 15 specimens (error bars for standard deviation not visible due to ordinate axis scale).

validates the modeling, thus suggesting potential for FEA-based design optimization in the future. Fig. 6 shows a typical MN device after mechanical testing. The graceful, plasticity-based failure mode suggests potential for greater safety and reliability than comparable needles made from conventional micromechanical materials, such as Si and SiO_2, whose intrinsic brittleness causes predisposition for catastrophic failure by fracture-based fragmentation.

B. MN Coating

Fig. 7 shows coated solid and fenestrated Ti MNs with identical shank dimensions. Uniform coating is evident in both cases, and deposition of continuous coatings within the fenestrations is observed. This suggests that the coating formulation provides adequate viscosity and wettability for the intended application. However, quantification of loading is not possible from these images, nor is it possible to determine the extent of fenestration filling. Consequently, it is not possible to determine whether the fenestrations increase loading capacity relative to solid MNs.

Our future studies will quantify drug loading using spectrofluorimetry, and this understanding will be used to inform subsequent coating formulation and deposition processes optimization efforts. Potential for delivery of controlled release vehicles will also be explored (e.g., biodegradable polymeric nanoparticles entrained in a fast-

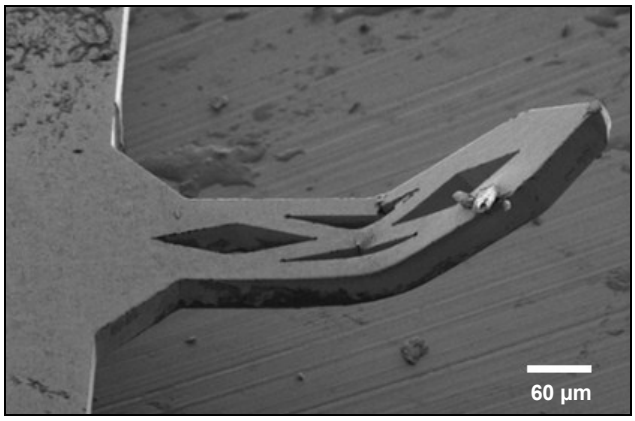

Fig. 6. Scanning electron micrograph of buckled Ti MN demonstrating graceful, plasticity-based failure mode.

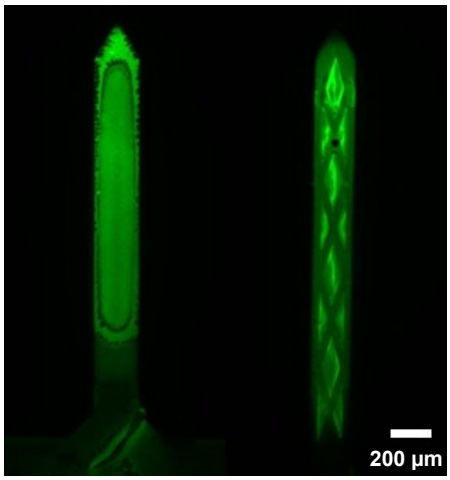

Fig. 7. Fluorescence micrographs of PVP/Lutrol F-68/Rhodamine B coated solid (left) and fenestrated (right) Ti MNs with identical shank dimensions (1500 x 200 x 50 μm^3).

dissolving coating), since this will provide opportunity for achieving sustained delivery, and, thus, reduced treatment frequency.

C. Ex Vivo Tissue Insertion

Fig. 8 shows histological confirmation of MN insertion into excised rabbit cornea. No damage to the MN was evident after removal (data not shown). The observed ~200 µm penetration depth is roughly half that of the MN length, due to tissue deformation prior to penetration. This is consistent with observations by others using solid, steel-based MNs [1]. These results demonstrate the potential embodied in MNs for precisely penetrating into, but not through cornea, thus enhancing safety relative to intravitreal injection. Moreover, the ability to achieve MN insertion manually (i.e. non-surgically) demonstrates the inherent simplicity of this approach.

Our future studies will seek to quantify insertion forces and scleral/corneal tissue toughness, and this understanding will be used to inform subsequent MN design optimization efforts focused on maximizing insertion reliability and drug loading while minimizing tissue trauma. Characterization of intrascleral/corneal drug transport from MNs will also be performed, first *in vitro*, and then *in vivo*. Data generated from these studies will be used to develop analytical models describing intrascleral and intracorneal drug diffusion, and these models will be used to inform both the design and the deployment strategy for fenestrated Ti MNs.

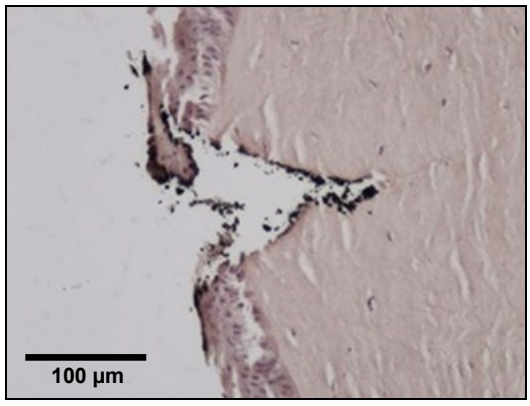

Fig. 8. Histological section of excised rabbit cornea at insertion site of 500 x 200 x 50 μm^3 MN (H&E stain).

V. Conclusion

We have reported the design, fabrication, and preliminary characterization of fenestrated Ti MNs for passive ocular drug delivery. Mechanical testing results demonstrate that these devices possess sufficient stiffness for reliable corneal insertion, and also provide potential for enhanced safety, due to their graceful, plasticity-based failure mode. Moreover, uniform deposition of a fast-dissolving model drug coating formulation on the fenestrated MNs has been demonstrated, although further studies are required to quantify drug loading capacity enhancement relative to comparable solid MNs. Finally, results from preliminary insertion studies in *ex vivo* cornea corroborate many of these findings by demonstrating capability for reliable MN insertion. Collectively, these results begin to demonstrate the potential embodied in fenestrated Ti MNs for providing a safe, simple, and efficacious means for targeted and sustained ocular drug delivery.

Acknowledgments

The authors thank Fady Hanna, Chris Salinas, and Steven Herrera for assistance with mechanical testing. The authors also acknowledge the University of California Riverside Regents' Faculty Fellowship for partial support of this work.

References

[1] J Jiang, HS Gill, D Ghate, BE McCarey, SR Patel, HF Edelhauser, and MR Prausnitz. Coated microneedles for drug delivery to the eye. *Invest Ophthalmol Vis Sci*, 48:4038-4043, 2007.

[2] J Jiang, JS Moore, HF Edelhauser, and MR Prausnitz. Intrascleral drug delivery to the eye using hollow microneedles. *Pharmaceut Res*, 26:395-403, 2009.

[3] SR Patel, ASP Lin, HF Edelhauser, and MR Prausnitz. Suprachoroidal drug delivery to the back of the eye using hollow microneedles. *Pharmaceut Res*, 28:166-176, 2011.

[4] ER Parker, MP Rao, KL Turner, CD Mienhart, and NC MacDonald. Bulk micromachined titanium microneedles. *J Microelectromech S* 16(2):289-95, 2007.

[5] PT McCarthy, KJ Otto, and MP Rao. Robust penetrating microelectrodes for neural interfaces realized by titanium micromachining. *Biomed Microdevices* 13(3):503-515, 2011.

[6] ER Parker, BJ Thibeault, MF Aimi, MP Rao, and NC MacDonald. Inductively coupled plasma etching of bulk titanium for MEMS applications. *J Electrochem Soc*, 152(10):C675-C683, 2005.

[7] HS Gill and MR Prausnitz. Coating formulations for microneedles. *Pharmaceut Res*, 24(7):1369-1380, 2007.

[8] JS Pulido, ME Zobitz, and K-N An. Scleral penetration force requirements for commonly used intravitreal needles. *Eye*, 21:1210-1211, 2007.